Journal of proteome research

Article

pubs.acs.org/jpr

Metabolic Markers of MG-63 Osteosarcoma Cell Line Response to Doxorubicin and Methotrexate Treatment: Comparison to Cisplatin

Inês Lamego,[†] Iola F. Duarte,[†] M. Paula M. Marques,[‡,§] and Ana M. Gil*[,†]

[†]CICECO−Departmento de Química, Universidade de Aveiro, Campus Universitário de Santiago, 3810-193 Aveiro, Portugal

[‡]R&D Unit "Molecular Physical-Chemistry" and [§]Department of Life Sciences, Faculty of Science and Technology, University of Coimbra, 3001-401 Coimbra, Portugal

Supporting Information

ABSTRACT: A high resolution magic angle spinning NMR metabolomics study of the effects of doxorubicin (DOX), methotrexate (MTX) and cisplatin (cDDP) on MG-63 cells is presented and unveils the cellular metabolic adaptations to these drugs, often used together in clinical protocols. Although cDDP-treated cells were confirmed to undergo extensive membrane degradation accompanied by increased neutral lipids, DOX- and MTX-treated cells showed no lipids increase and different phospholipid signatures, which suggests that (i) DOX induces significant membrane degradation, decreased membrane synthesis, and apparent inhibition of *de novo* lipid synthesis, and (ii) MTX induces decreased membrane synthesis, while no membrane disruption or *de novo* lipid synthesis seem to occur. Nucleotide signatures were in apparent agreement with the different drug action mechanisms, a link having been found between UDP-GlcNAc and the active pathways of membrane degradation and energy metabolism, for cDDP and DOX, with a relation to oxidative state and DNA degradation, for cDDP. Correlation studies unveiled drug-specific antioxidative signatures, which pinpointed *m*- and *s*-inositols, taurine, glutamate/glutamine, and possibly creatine as important in glutathione metabolism. These results illustrate the ability of NMR metabolomics to measure cellular responses to different drugs, a first step toward understanding drug synergism and the definition of new biomarkers of drug efficacy.

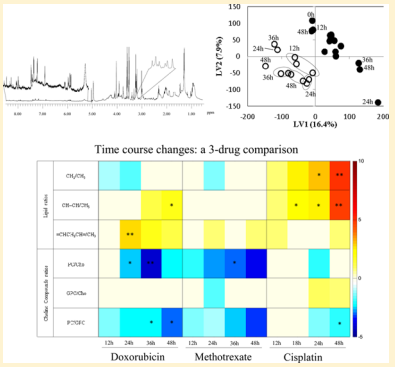

KEYWORDS: *osteosarcoma, MG-63 cell line, cisplatin, doxorubicin, methotrexate, cancer, chemotherapy, metabolomics, NMR spectroscopy*

INTRODUCTION

Metabolic profiling of cultured cancer cells when exposed to drugs enables cellular metabolic response to be measured, which offers valuable insight into drug mechanisms at the cellular level and, ultimately, drug efficacy and toxicity. Although extrapolation of cell studies to *in vivo* conditions is far from straightforward, *in vitro* assays benefit from a finer control of growth conditions and ease of interpretation of metabolic results, which thus provides information concerning the first level of drug effects on the metabolism of cancer cells and enables potential novel markers of drug performance to be identified. Such metabolic markers are good candidates for *in vivo* testing, for instance, through magnetic resonance imaging, some eventually contribute to improved management protocols of chemotherapy response. Cell metabolomics uses analytical methodologies with large compound resolution power, such as mass spectrometry (MS) and ^{1}H nuclear magnetic resonance (NMR) spectroscopy; the latter allows the metabolome of cultured cells (down to sub-mM concentrations) to be characterized rapidly, noninvasively, and with high reproducibility. NMR metabolomics may handle either cell extracts or pellets through liquid state and high resolution magic angle spinning (HRMAS) NMR, respectively, and a vast number of studies have been reported on different mammalian cells exposed to drugs known to act through different mechanisms.[1−3]

The present study deals with the effects of doxorubicin (DOX), methotrexate (MTX), and cisplatin (cDDP) (Figure 1) on the human osteosarcoma (OS) MG-63 cell line. These three agents (often together with ifosfamide) are the components of one of the most commonly adopted preoperative chemotherapy

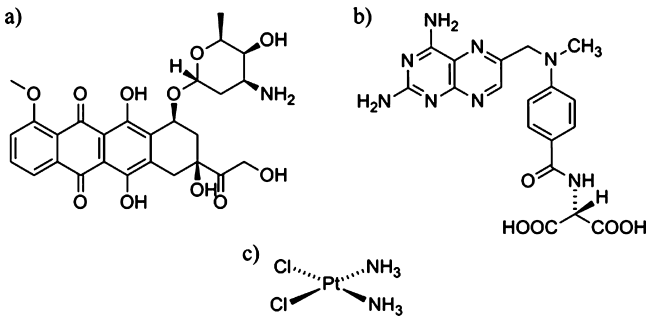

Figure 1. Chemical structures of DOX, MTX, and cDDP.

Received: September 1, 2014
Published: November 10, 2014

regimen for the treatment of nonmetastatic high grade OS,[4,5] a frequent type of malignant bone tumor in pediatric and adolescent age groups.[6] Although much knowledge is available on the specific mechanisms of action of DOX (cytostatic, intercalates with DNA thus preventing replication),[7] MTX (cytostatic, interferes with the natural folate-homocysteine cycle and with purine *de novo* synthesis),[8] and cDDP (cytotoxic, forms intra- and interstrand DNA cross-links),[9−12] relatively little is known on the metabolic adaptations of tumor cells to each drug and on the occurrence of possible metabolic markers of drug efficacy. In this respect, cDDP has been more extensively investigated by metabolomics, mainly NMR-based, in several cancer cells: lung,[13,14] brain,[15−17] liver,[18] and OS,[19] the latter by our own group. Regarding DOX, NMR metabolomics has been used for leukemia cell lines,[20−24] colorectal[22] and breast cancers,[25,26] and melanoma.[27] To the best of our knowledge, no NMR metabolomics studies have been reported on MTX effects in neoplasic cell lines in addition to existing MS studies using leukemia,[28] cervical,[29] colon,[30] and breast cancers.[25] It becomes apparent, therefore, that studies on OS cells exposed to DOX or MTX are presently lacking, either by NMR or MS metabolomics, which justifies the present work.

In this work, ^{1}H HRMAS NMR spectroscopy was used to investigate changes in the metabolic profile of MG-63 OS cells treated with DOX and MTX; these results were compared with those previously reported for cDDP on the same cell line.[19] The latter results were reprocessed by improved methodologies (spectral alignment and probabilistic quotient normalization), thus the effects of cDDP on MG-63 cells were reassessed, and clearly the importance of the data processing protocol was evidenced. The application of multivariate analysis to the ^{1}H HRMAS NMR spectra of cell pellets, recorded for both controls and drug-treated cells, enabled drug-specific variation patterns to be identified, while spectral integration of relevant signals provided a quantitative measurement of the time course variations of the cells' metabolome. Overall, the interdrug comparison presently reported offers an integrative picture of MG-63 OS cell response to different chemotherapeutic agents, which enables specific metabolic signatures of cellular response to be unveiled and explanatory biochemical hypothesis of drug response to be discussed.

EXPERIMENTAL SECTION

Chemicals

(3-(4,5-Dimethylthiazolyl-2)-2,5-diphenyltetrazolium bromide (MTT), phosphate buffered saline (PBS, pH 7.4), dimethyl sulfoxide (DMSO), Eagle's minimum essential medium (MEM), trypsin solution, and cell media components were obtained from Sigma-Aldrich. Fetal bovine serum (FBS) was purchased from Gibco. Stock solutions of DOX and MTX (Fisher Scientific) were prepared in Milli-Q H_2O and DMSO, respectively, to 3 mM concentrations, made sterile through filtration (0.22 μm syringe filter), and stored at 4 °C. For cDDP assays, chemicals are described elsewhere.[19]

Cell Culture and Drug Administration

The human MG-63 OS cell line was kindly provided by the Associate Laboratory IBMC-INEB, Portugal. Cells were grown as monolayers in MEM culture medium, supplemented with 10% heat-inactivated FBS, 1 mM sodium pyruvate, nonessential amino acids (1 mM) and antibiotics (penicillin-streptomycin 100x), and maintained under a humidified atmosphere with 5% CO_2 at 37 °C.

Cells were harvested 96 h after seeding upon addition of trypsin (0.05% trypsin/EDTA solution) and plated in 100 mm diameter Petri dishes (~5×10^6 cells per dish). After waiting 24 h for cells to adhere, the experiment was initiated (t = 0 h) by adding 12 μL DOX or MTX 3 mM stock solutions to each Petri dish (containing 12 mL MEM) in order to achieve a final drug concentrations of 3 μM. This concentration corresponds to the IC_{50} value determined (by the MTT assay) for both drugs at 24 h (results not shown). Distinct control samples were considered for each compound, 12 μL of Milli-Q H_2O and 12 μL of DMSO (to ensure MTX solubility) having been added to the controls, respectively, for DOX and MTX experiments. The adherent cells were harvested by trypsinisation, at t = 12, 24, 36, and 48 h, washed with PBS (pH 7.4), and centrifuged (for 6 min, at 1000 rpm, 21 °C). The resulting cell pellet was suspended in 1 mL PBS/D_2O (0.14 M NaCl, 0.0027 M KCl, 0.0015 M KH_2PO_4, 0.0081 M Na_2HPO_4 in deuterated water, pH 7.4), centrifuged, and resuspended in 35 μL PBS/D_2O, to which 5 μL of PBS/D_2O containing TSP 0.25% (for chemical shift referencing) was added. Then, a three-fold cycle of liquid nitrogen dipping and sonication was performed to obtain a suspension of lysed cells. Each sample was then transferred to a sealed NMR disposable insert (ca. 35 μL) and stored at −80 °C until analysis. Three independent assays with duplicates for each condition (time point and drug dosage) were performed for cell passages between 25 and 29. For NMR analysis, the duplicates were mixed when necessary to provide samples with a large enough number of cells (ideally between 5 and 10×10^6 cells) for good signal-to-noise spectra to be obtained. For cDDP assays, procedures were those described elsewhere[19] for an IC_{50} value (at 24 h) of 30 μM.

Cell Viability Assays

IC_{50} measurements for DOX and MTX were performed by the MTT colorimetric assay,[31,32] which is based on the spectrophotometric detection of the reduction of the yellow methylthiazolotetrazolium salt to the violet formazanby, the mitochondrial oxidoreductase enzymes of living cells. Cells were plated on 24-well plates at 1×10^5 cells per well. Cells were treated, 24 h later, with increasing doses of DOX (0.1, 1, 3, and 6 μM) and MTX (0.1, 0.5, 1, 3, and 5 μM) added to the cultures, and these were incubated in a humidified atmosphere at 37 °C and 5% CO_2. After 24 h of exposure, cells were washed with 1 mL of PBS before 250 μL of MTT solution (0.5 mg/mL in PBS) was added and were incubated for 3 h at 37 °C. The violet MTT formazan precipitate was solubilized by adding 500 μL of DMSO, and absorbance was measured at 570 nm in a microplate reader. Experiments were performed in triplicates. Absorbance of control cells was taken as 100% viability, and the values of treated cells were calculated as a percentage of the control. For NMR experiments at each time point, the extent of cell death was assessed using the Trypan blue exclusion assay, which yields the number of living versus dead cells and thus provides a measure of cell membrane integrity. Briefly, cells were incubated with Trypan blue dye (0.4% (w/v) solution in PBS) and counted in a Neubauer-counting chamber. Numbers of living (dye-excluding) cells were expressed in terms of mean ± standard error of the mean.

NMR Measurements

The disposable inserts containing the cell samples were placed in standard 4 mm MAS rotors and analyzed on a Bruker Avance spectrometer operating at 800.33 MHz for ^{1}H observation, at 277 K, using a 4 mm HRMAS probe, in which the rotor containing the sample was spun at the magic angle and a 4 kHz

dx.doi.org/10.1021/pr500907d | J. Proteome Res. 2014, 13, 6033−6045

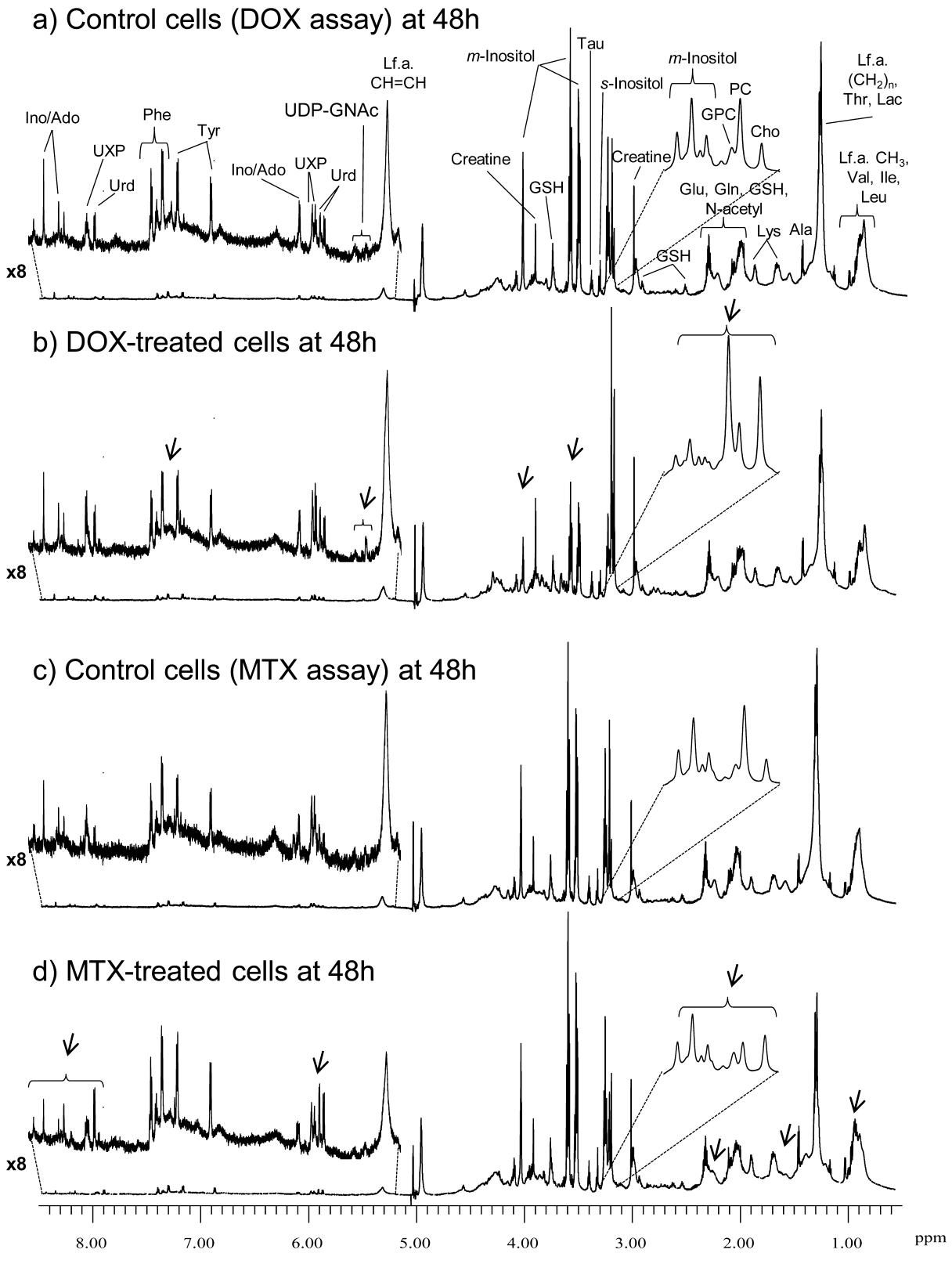

Figure 2. Average 800 MHz ^{1}H HRMAS NMR spectra of MG-63 cells at 48 h: (a) under control conditions (assay of exposure to DOX); (b) exposed to 3 μM DOX; (c) under control conditions (assay of exposure to MTX); and (d) exposed to 3 μM MTX. Insets show expansions of choline compounds (3.2−3.3 ppm) and aromatic (5.15−8.5 ppm) regions. Main assignments are noted: three-letter code used for amino acids; Cho, choline; GPC, glycerophosphocholine; GSH, reduced glutathione; Lac, lactate; L.f.a., lipid fatty acyl groups; PC, phosphocholine; PE, phosphoethanolamine; Tau, taurine; UDP-GNAc, uridine diphosphate acetylhexosamine; Urd, uridine; UXP, either of UDP/UTP/UDP-GNAc species. Arrows in panels b and d indicate visible spectral changes due to drug exposure.

dx.doi.org/10.1021/pr500907d | J. Proteome Res. 2014, 13, 6033−6045

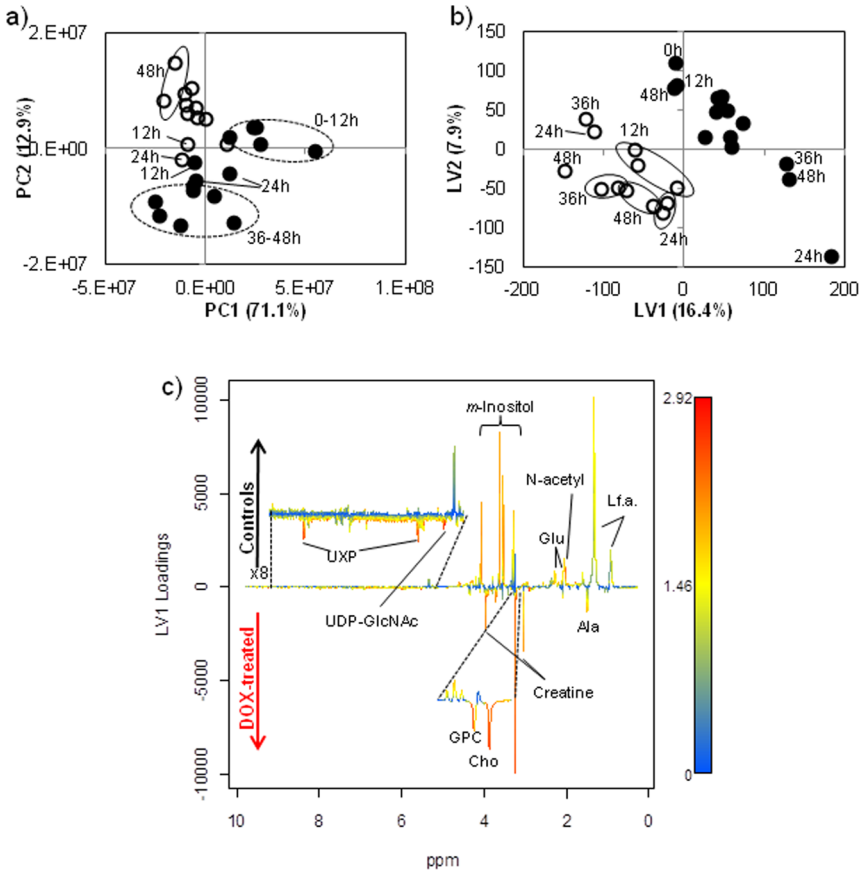

Figure 3. Multivariate analysis of 800 MHz ^{1}H HRMAS spectra of MG-63 control cells (●) and MG-63 cells exposed to 3 μM DOX (○): (a) PCA scores scatter plot (PC1 vs PC2, centered scaled data); (b) PLS-DA scores scatter plot (LV1 vs LV2, unit variance (UV) scaled data), LV = 2, R^2X = 0.243, R^2Y = 0.918, and Q^2 = 0.665; (c) PLS-DA LV1 loadings plot, colored as a function of VIP value, and peak labeling as defined in Figure 2 caption.

spinning rate. The spectra obtained for cDDP exposure studies have been recorded at a field strength of 700 MHz in similar conditions.[19] A standard 1D spectrum (pulse program "noesypr1d", Bruker library) was acquired for each sample, with spectral width of 9803.92 Hz, 32 K data points, 100 ms mixing time, 4 s relaxation delay, and 256 scans. All 1D spectra were processed with a line broadening of 0.3 Hz and zero filling to 64 K, manually phased, and baseline corrected. Chemical shifts were referenced internally to the alanine signal at δ 1.48. Spectral assignment was based on 2D total correlation spectroscopy (TOCSY), heteronuclear single quantum coherence (HSQC) spectra, and consultation of spectral databases (Bruker Biorefcode database and the human metabolome database, HMDB)[33] and further supported by statistical total correlation spectroscopy (STOCSY)[34] (MATLAB version 7.12.0, The MathWorks Inc.).

Data Processing and Analysis

A total of 50 spectra were acquired, comprising 26 control samples, 12 DOX-treated samples, and 12 MTX-treated samples. One of the MTX-treated samples revealed an abnormally strong profile of lipid resonances, and for this reason it was not considered for multivariate analysis. In addition, the spectra obtained in an earlier study[19] of MG-63 cells (same cell line) exposed to cDDP were reprocessed, as described next. Data matrices were built from standard 1D spectra (δ 0.25−9.80), excluding the water region (δ 4.9−5.1), and spectra were aligned using recursive segment wise peak alignment[35] to minimize chemical shift variations and were normalized to probabilistic quotient normalization (PQN)[36] to account for dilution-independent effects on spectral area (MATLAB version 7.12.0, The MathWorks Inc.). After scaling (unit variance or mean centering), principal component analysis (PCA) and partial least squares regression discriminant analysis (PLS-DA) were applied separately to each set of spectra corresponding to each drug assay (MTX, DOX, and cDDP) using SIMCA -P 11.5 (Umetrics, Sweden) and employing Monte Carlo Cross-Validation (MCCV) through a default seven-fold internal cross validation, from which Q^2 (predictive ability) and R^2 (explained variance) values were extracted. To evaluate the magnitude of variation of some compounds, selected signals in the 1D spectra were integrated (using Amix-Viewer software, Bruker, version 3.9.11), and % variation was calculated as 100 (mean integral in drug-treated samples − mean integral in controls)/mean integral in controls. Effect size values were calculated as described elsewhere, with a correction factor for low number of samples.[37] For each metabolite, the statistical significance of the difference between the means of the two groups (control and treated) was assessed using the two-sample t test. A p-value <0.05 (confidence level 95%) was considered for statistical significance. Unidimensional STOCSY[34] was performed in Matlab 7.12.0 for assignment and search of metabolic correlations.

RESULTS

The average ^{1}H HRMAS spectra of control and DOX-treated MG-63 cells, at 48h, are shown in Figure 2, panels a and b, respectively. Visual inspection reveals marked changes in the choline region (relative increases in choline, Cho, and

dx.doi.org/10.1021/pr500907d | J. Proteome Res. 2014, 13, 6033−6045

Table 1. Metabolite Variations in MG-63 Cells Exposed to 3 μM DOX, 3 μM MTX, and 30 μM cDDP for 48 h Compared to Control Cells. Ado, Adenosine; GPC, Glycerophosphocholine; GSH, Gluthathione; Ino, Inosine; PC, Phosphocholine; PE, Phosphoethaloamine; UDP-GlcNAc, Uridine Diphosphate Glucosamine; UXP, UDP and/or UTP and/or UDP-GNAc, where UDP-GNAc, Uridine Diphosphate Hexosamine; UDP, Uridine Diphosphate; UTP, Uridine Triphosphate

		doxorubicin (DOX)		methotrexate (MTX)		cisplatin (cDDP)[b]	
metabolite	signal (δ/ppm)[a]	% var.[c]	effect size[d]	%var.[c]	effect size[d]	% var.[c]	effect size[d]
Lipids							
-C$\underline{H}_3$	0.91	_	_	_	_	42.2 ± 3.0**	8.88 ± 2.46
-(C$\underline{H}_2$)$_n$	1.30	_	_	_	_	115.6 ± 2.4**	20.0 ± 5.40
-C$\underline{H}_2$C-H$_2$CO	1.60	_	_	_	_	47.1 ± 4.1**	7.24 ± 2.04
-C$\underline{H}_2$CO-O	2.25	_	_	_	_	41.8 ± 3.4**	6.98 ± 1.97
=CHC-$\underline{H}_2$C-H=	2.83	53.4 ± 10.5*	2.63 ± 1.00	8.20 ± 3.30	1.59 ± 0.83	61.1 ± 12.6	2.88 ± 1.00
-C$\underline{H}$=C$\underline{H}$-	5.33	(+)	(+)	_	_	228.1 ± 9.6**	9.14 ± 2.52
Choline and Phospholipids							
choline	3.21, s	178 ± 15.4*	3.94 ± 1.31	41.1 ± 16.0	1.26 ± 0.78	32.7 ± 6.4**	2.88 ± 1.00
GPC	3.24, s	266 ± 39.0	1.91 ± 0.86	(+)	(+)	213 ± 55.3	1.55 ± 0.76
PC	3.23, s	−28.6 ± 12.3	−1.77 ± 0.83	−56.4 ± 17.2	−3.91 ± 1.40	_	_
PE	3.25, t	(+)	(+)	(+)	(+)	−19.0 ± 5.5*	−2.67 ± 0.96[e]
Amino acids							
alanine	1.40, d	_	_	_	_	−8.40 ± 1.90**	−2.91 ± 1.01
glutamate	2.34, m	_	_	−21.6 ± 9.8	−1.54 ± 0.82	−27.7 ± 6.2**	−2.79 ± 0.98
glycine	3.56, s	−28.0 ± 13.6	−1.57 ± 0.80	24.4 ± 6.9	1.60 ± 0.84	−35.6 ± 9.0**	−2.73 ± 0.97
histidine	8.18, s	_	_	(+)	(+)	(+)	(+)
isoleucine	1.02, d	_	_	_	_	12.3 ± 5.1	1.75 ± 0.80
leucine		_	_	_	_	−10.0 ± 2.9*	−2.10 ± 0.85
lysine	1.72, m	(−)	(−)	_	_	−12.6 ± 3.9*	−2.04 ± 0.84
phenylalanine	7.32, d	_	_	17.6 ± 4.2*	2.05 ± 0.93	−23.0 ± 4.1**	−3.91 ± 1.23
proline	4.12, t	_	_	_	_	−10.1 ± 5.8	−1.12 ± 0.71[e]
taurine	3.42, t	(−)	(−)	−12.5 ± 4.1	−1.76 ± 0.87	(−)	(−)
threonine	3.58, d	(−)	(−)	_	_	(−)	(−)[e]
tyrosine	6.89, d	27.2 ± 8.8	1.78 ± 0.83	26.6 ± 5.7	2.06 ± 0.93	−19.9 ± 7.1*	−1.99 ± 0.83
valine	1.05, d	_	_	(+)	(+)	12.0 ± 5.3	1.59 ± 0.77
Nucleotides and Derivatives							
Ado/Ino	8.36, s	_	_	_	_	−38.2 ± 8.1**	−3.41 ± 1.12
UDP-GlcNAc	5.52, m	166 ± 32.6	1.36 ± 0.80	_	_	66.4 ± 28.9	1.13 ± 0.73[e]
UXP	5.99, m	_	_	(−)	(−)	155 ± 40.1	1.63 ± 0.78[e]
	7.98, m	(+)	(+)	_	_	77.3 ± 21.3*	1.72 ± 0.79
uridine	5.89, d	(+)	(+)	165.4 ± 54.5	0.94 ± 0.73	_	_
Other Compounds							
Acetate (s)	2.02, s	_	_	_	_	27.5 ± 4.7**	3.17 ± 1.06
creatine	3.93, s	13.7 ± 6.1	1.37 ± 0.76	−10.7 ± 3.7	−2.28 ± 0.98	_	_
GSH (red.)	2.56, m	−20.3 ± 7.6	−1.94 ± 0.86	(−)	(−)	_	_
m-inositol	4.05, t	−53.0 ± 10.9*	−4.34 ± 1.41	_	_	−60.7 ± 13.9**	−3.30 ± 1.09
s-inositol	3.34, s	−22.1 ± 8.3*	−1.96 ± 0.86	_	_	−37.8 ± 8.9**	−2.84 ± 1.00

[a]Resonance chosen for signal integration: s, singlet; t, triplet; d, doublet; m, multiplet. [b]Values based on previously reported data,[19] hereby reprocessed and reanalyzed. [c]% Variation. [d]Effect size in relation to control cells. *, $p < 0.05$; **, $p < 0.01$; –, no significant variation. [e]Newly observed changes, compared to literature.[19]

glycerophosphocholine, GPC), a relative decrease in *m*-inositol, and some changes above 5 ppm. On the other hand, exposure to MTX, for 48h (Figure 2c,d), seems to affect the cellular metabolome differently in relation to lipids (see arrows at low ppm in Figure 2d), choline compounds (relative decrease in phosphocholine, PC, and possible increase in Cho), UXP (either of UDP/UTP/UDP-GNAc species), uridine, and other resonances at lower field (ca. 8 ppm). Comparison of the above effects with the reprocessed spectra of MG-63 cells exposed to cDDP (Figure S1a,b, Supporting Information),

dx.doi.org/10.1021/pr500907d | J. Proteome Res. 2014, 13, 6033−6045

Table 2. Mean Peak Ratios for Lipids and Choline Compounds in MG-63 Cells Exposed to 3 μM DOX, 3 μM MTX, and 30 μM cDDP for 48 h Compared to Control Cells. Abbreviations as Defined in Table 1. * $p < 0.05$, ** $p < 0.01$

	doxorubicin (DOX)		methotrexate (MTX)		cisplatin (cDDP)	
ratio	controls	DOX	controls	MTX	controls	cDDP
Lipid Ratios						
$\underline{CH_2}/\underline{CH_3}$	2.59 ± 0.24	2.36 ± 0.12	2.58 ± 0.28	2.05 ± 0.21	1.96 ± 0.08	2.97 ± 0.12**
$\underline{CH}{=}\underline{CH}/\underline{CH_3}$	0.19 ± 0.02	0.29 ± 0.04*	0.20 ± 0.04	0.16 ± 0.02	0.11 ± 0.01	0.26 ± 0.02**
$=CHC\underline{H_2}CH=/\underline{CH_3}$	0.20 ± 0.06	0.31 ± 0.01	0.18 ± 0.04	0.25 ± 0.02	0.20 ± 0.01	0.22 ± 0.02
Choline Compound Ratios						
PC/Cho	2.18 ± 0.64	0.56 ± 0.15	2.68 ± 0.46	0.83 ± 0.08	2.17 ± 0.60	1.72 ± 0.29
GPC/Cho	1.17 ± 0.22	1.55 ± 0.42	0.92 ± 0.02	0.86 ± 0.19	0.38 ± 0.04	0.91 ± 0.44
PC/GPC	1.86 ± 0.52	0.36 ± 0.18*	2.92 ± 0.56	0.97 ± 0.16	5.63 ± 1.45	1.90 ± 0.99*

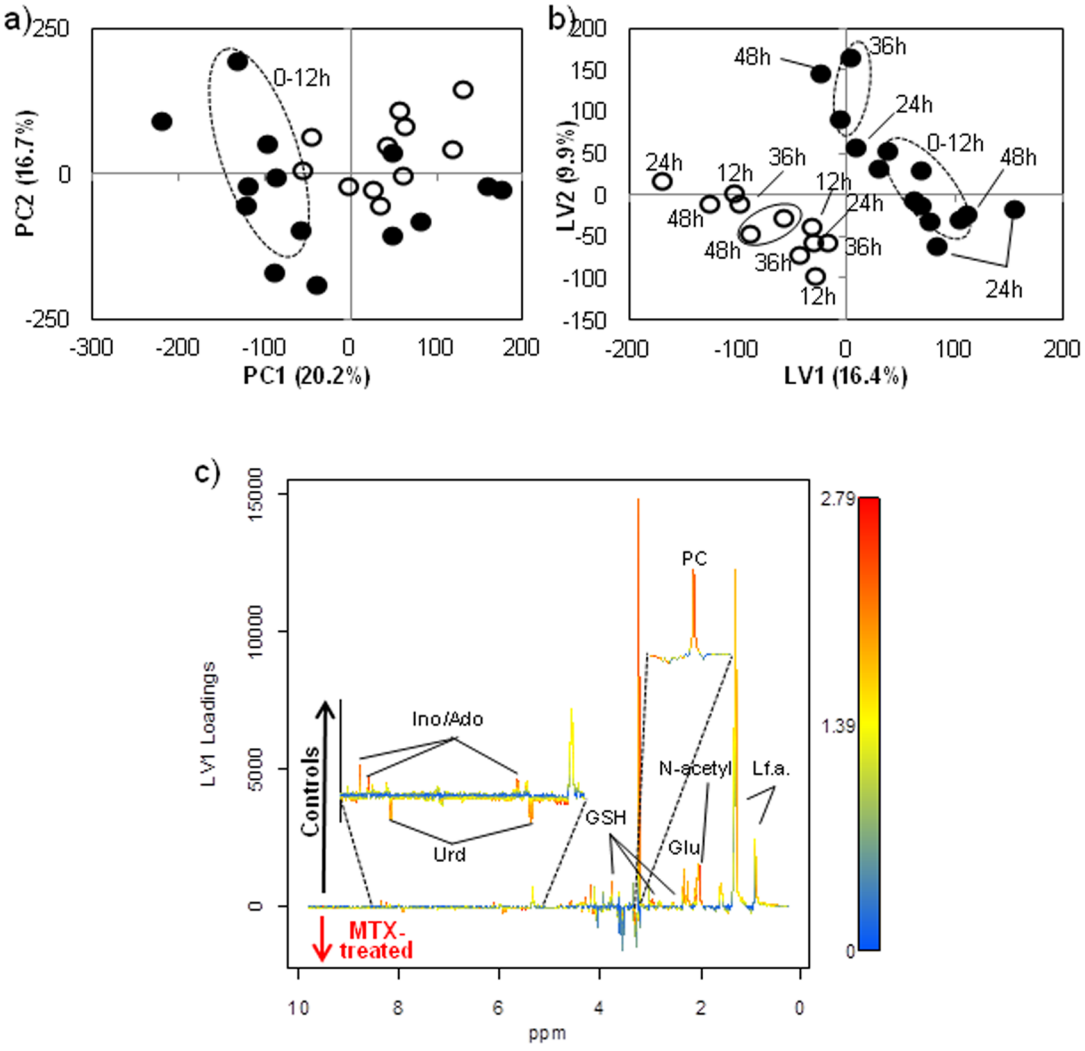

Figure 4. Multivariate analysis of 800 MHz ^{1}H HRMAS spectra of MG-63 control cells (●) and MG-63 cells exposed to 3 μM MTX (○): (a) PCA scores scatter plot (PC1 vs PC2, UV scaled data); (b) PLS-DA scores scatter plot (LV1 vs LV2, UV scaled data), LV = 2, $R^2X = 0.262$, $R^2Y = 0.902$, and $Q^2 = 0.622$; (c) PLS-DA LV1 loadings plot, colored as a function of VIP value, peak labeling as defined in Figure 2 caption.

clearly indicated that (1) the marked lipids increased characteristic of apoptotic response to cDDP is absent in both DOX- and MTX-treated cells, and (2) response to cDDP is distinct from those induced by DOX and MTX in terms of choline compounds, nucleotide bases, and acetylglycosylated derivatives (above 5 ppm).

To confirm visual observations and unveil the most relevant changes, multivariate analysis was applied to the ^{1}H HRMAS spectra of controls and drug-treated cells. PCA resulted in a clear separation between DOX-treated cells and controls, toward negative PC1 and positive PC2 (Figure 3a). Although a time course tendency was suggested for control samples in PCA, such was only faintly noted for DOX-treated cells. The corresponding PLS-DA scores plot (Figure 3b) showed good separation between groups (Q^2 0.665), although time course tendencies were again unclear. The robustness of group discrimination was reflected in a low Q^2 distribution overlap and reasonable MCCV results (83% sensitivity, 90% specificity, and 87% classification

dx.doi.org/10.1021/pr500907d | J. Proteome Res. 2014, 13, 6033−6045

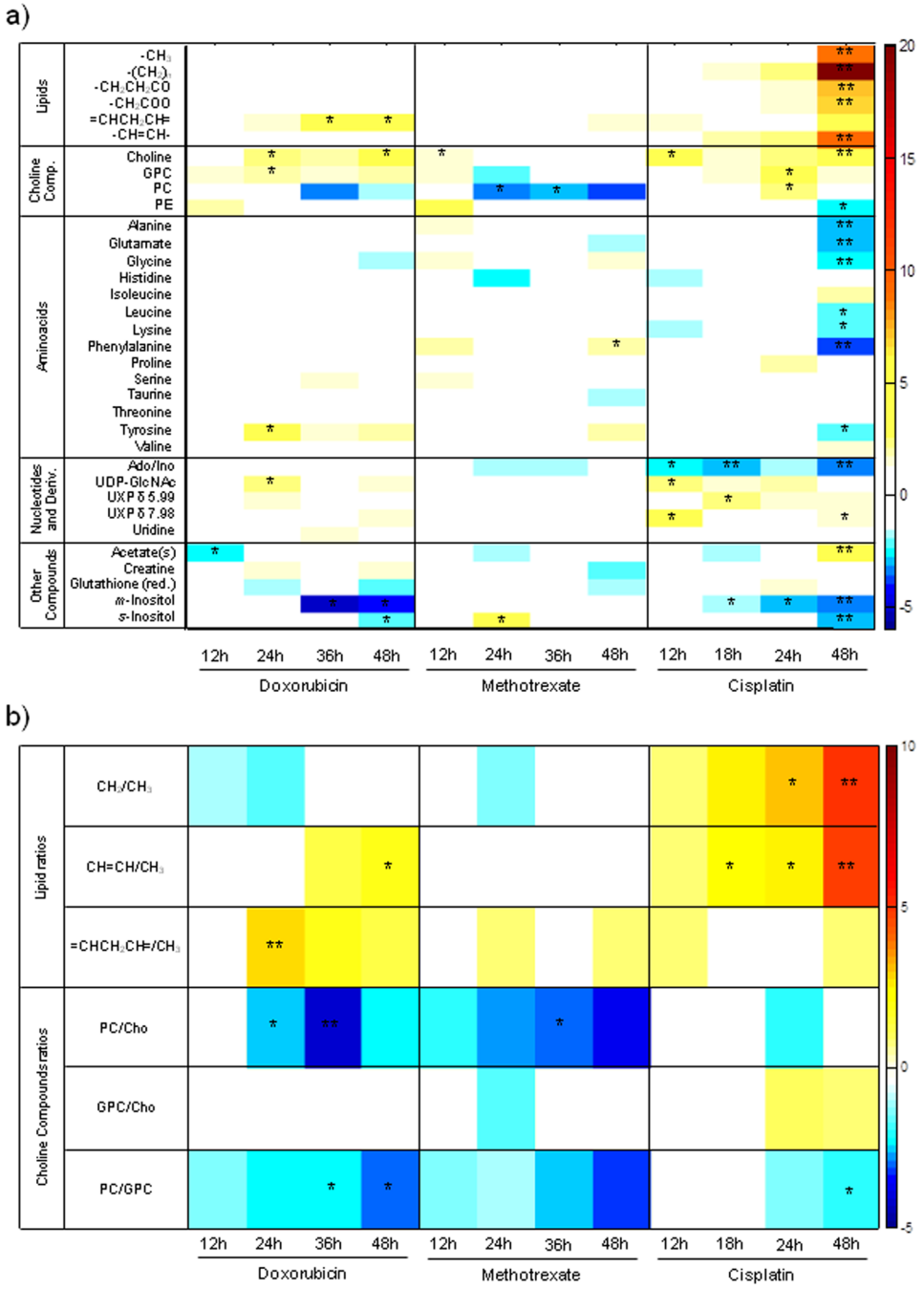

Figure 5. Heatmaps of effect size values of the time-course response of (a) several metabolites and (b) peak ratios in MG-63 cells exposed to DOX, MTX, and cDDP. Effect size values are shown in a color scale from minimum (dark blue) to maximum (dark red) values.

rate) (Figure S5a,b). The VIP-colored loadings (Figure 3c) gave a qualitative idea of what metabolites are responsible for group separation upon DOX exposure, which suggests the importance of *m*-inositol, choline compounds, creatine, and nucleotides. Subsequent signal integration (generally using fixed spectral intervals and, in the cases of choline compounds and N-acetyl resonances, using signal deconvolution) and statistical evaluation identified the relevant variations, comprised in Table 1 for 48 h and shown in time-course plots in Figure S2. These results indicated a metabolite profile of response of MG-63 cells to DOX described by (1) residual changes in lipids, with small increases in $=CHCH_2CH=$ and $-CH=CH-$ resonances at 48 h (Table 1), also expressed by $=CHCH_2CH=/CH_3$ and $-CH=CH-/CH_3$ lipid ratios (Table 2); (2) marked increases in Cho and GPC in tandem with PC decrease (Table 1, Figure S2a), resulting in significant decreases in PC/Cho and PC/GPC ratios (Table 2, Figure S2b); (3) large Gly decrease and Tyr increase (Table 1, Figure S2a) accompanied by a slight decrease tendency in other amino acids (Table 1); (4) marked increase in UDP-GlcNAc at 24 h (not shown) and 48 h (Table 1) and small increases in UXP and uridine; and (5) significant increase in creatine and decreases in GSH and *m*- and *s*-inositols (Table 1, Figure S2a).

Regarding MG-63 response to MTX, group separation was less obvious in the PCA scores plot (Figure 4a) but clear, again, in the corresponding PLS-DA scores plot (Figure 4b). MCCV

dx.doi.org/10.1021/pr500907d | *J. Proteome Res.* 2014, 13, 6033−6045

performance was slightly lowered (Figure S5c,d), which suggests an overall lesser impact of the drug on the cell metabolome compared to DOX. The VIP-loadings (Figure 4c) indicated a distinct response profile, namely in the choline region (clear decrease in PC) and nucleotide bases region. Signal integration (Table 1, Figure S3) indicated the following: (1) nearly absent lipid changes; (2) almost no changes in Cho and GPC (except for small increases at 48 h) and a large decrease in PC, which thus decreased PC/Cho and PC/GPC ratios markedly (Table 2, Figure S3b); (3) increases in Gly, Phe, Tyr and decreases in Glu and Tau; (4) large increase in uridine, although with large uncertainty in effect size value; and (5) small decrease in creatine, along with a weak decreasing tendency for GSH and no changes in inositols. The above observations clearly show that MG-63 OS cells respond quite differently to DOX and MTX in terms of their metabolic adaptations.

In comparison, the metabolic effects resulting from MG-63 exposure to cDDP were confirmed to be significantly stronger, as seen by the quality of the corresponding PLS-DA model (Figures S1d and S5e,f), VIP-colored loadings (Figure S1e), the resulting list of statistically relevant metabolite changes at 48 h (Table 1), and as a function of time (Figure S4). As explained before, the results relating to cDDP were obtained through improved processing of the spectra previously reported,[19] namely peak alignment (which improved the MVA models for 30 μM cDDP/MG-63) and PQN normalization rather than normalization to total area, in order to more accurately correct for different cell numbers in different samples while important changes in spectral profile (namely those determined by the large lipid increase) and, hence, total area, were accommodated. Although most previously reported changes were confirmed (Table 1), some were now shown to be irrelevant (namely regarding creatine, PC, succinate, taurine), and some were newly unveiled (Pro, Thr, phosphoethanolamine (PE), UDP-GlcNAc, and UXP, marked with *e* in Table 1). General observations for cDDP response (Table 1, Figure S4) comprise: (1) significant increases in lipids content, average chain length, and unsaturation degree (respectively given by $(CH_2)_n/CH_3$ and $HC{=}CH/CH_3$, Table 2, Figure S4b; (2) increases in Cho and GPC and no change in PC, leading to decreased PC/Cho and PC/GPC ratios (Table 2, Figure S4b), while PE decreases; (3) large number of responding amino acids showing a general decreasing tendency (with the exception of Ile and Val); (4) changes in UXP and glucosylated derivatives (newly observed); and (5) marked decreases in *m*- and *s*-inositols similarly to DOX-treated cells, in addition to an increase in acetate(s).

A heatmap of effect size values (Figure 5a) expresses the most relevant time course changes, with hot and cold colors expressing, respectively, increased and decreased metabolite levels compared to controls. The numerous yellow/orange patches in the lipid resonances are a clear signature of cDDP response, whereas smaller and fewer changes are noted for the other two drugs, with even weak suggestions of decreases in the main lipid resonances. The increase in polyunsaturated fatty acids (PUFA) is a common feature to the three drugs, although more marked for DOX (even though total visible lipids do not increase) compared to cDDP and MTX. Regarding phospholipid-related compounds, drug-specific highlights include PE decrease for cDDP, marked PC decrease for MTX, and a mixed behavior for DOX (PC decrease and Cho and GPC increases). The ratios heatmap (Figure 5b) clearly shows the time course increase in lipid chain length and unsaturation degree in response to cDDP, along with a suggestion of chain length shortening for DOX and MTX in the former case (DOX) accompanied by some increase in unsaturations, including PUFA structures. The distinct choline signatures noted in Figure 5, panel (a) gain weight when PC/Cho and PC/GPC ratios are considered (Figure 5b). cDDP affects these ratios to a much lesser extent than do DOX and MTX, the latter induces a clearly gradual time course response in both ratios. This result identifies choline ratios as particularly sensitive markers of MG-63 metabolic response to DOX and MTX.

Regarding amino acids, color distribution for the three drugs is quite distinct: for cDDP, blue patches (decreases) predominate, especially at 48 h, whereas yellow patches (increases) predominate for DOX and MTX responses. The nucleotide base signatures also seem complementary, with more pronounced changes observed for cDDP (Ado/Ino decrease and increases in uridine nucleotide species), whereas DOX and MTX cause, respectively, small increases (yellow) and decreases (blue) in these compounds (note that for MTX, the uridine variation at 48 h (Table 1) does not feature in the heatmap because of the high effect size uncertainty). Regarding other compounds, the concomitant decreases in *m*- and *s*-inositols, which characterize cDDP and DOX responses, are totally absent in MTX, and distinct trends are seen for acetate(s), creatine, and GSH (with only a small increase for cDDP at 24 h and decreases for DOX and MTX).

DISCUSSION

Exposure to 3 μM DOX or 3 μM MTX (IC_{50} concentrations at 24 h) produced a much weaker metabolic response from MG-63 cells than did exposure to 30 μM cDDP (IC_{50} at 24h). In the following discussion, cDDP response will be taken as reference for subsequent comparison with the remaining two drugs tested, addressing the impacts on the metabolic pathways associated with lipids and choline-compounds, amino acids, nucleotides, and other compounds.

Lipids and Choline Compounds

Some of the main differences between MG-63 cell responses to the three drugs relate to lipids and choline compounds. The significant lipids increase observed as a response to cDDP was expected from previous studies, not only on OS cells,[19] but also on other tumor lines.[13,14,16,17] NMR-visible lipid signals are believed to arise mainly from cytosolic lipid droplets (composed of mobile neutral lipids), rather than membrane components,[38,39] but possible contributions from membrane lipid microdomains or lipid rafts have been suggested.[26,40] Increases in neutral lipid signals have been associated with cell apoptosis,[13,24,41] although some authors advance that they may also be due to other (still unclear) origins.[42−44] Specifically, it has been proposed that apoptosis involves inhibition of mitochondrial fatty acid β-oxidation and divertion of fatty acids to increased *de novo* lipid synthesis,[41] thus leading to an increase of the corresponding NMR-visible signals. Increased average chain length and unsaturation degree, as clearly confirmed here for MG-63 cells exposed to cDDP, have also been suggested as apoptosis signs.[13,45] The PUFA structures, detected here for the first time in cDDP-treated OS cells through the $=CHCH_2CH=$ resonance (60% increased upon cDDP treatment for 48 h), have been specifically suggested as preapoptotic functional lipid mediators in the cell death pathway.[17] Remarkably, MG-63 cells exposed to DOX or MTX failed to exhibit an increase in neutral lipids main resonances, CH_3 and $(CH_2)_n$ (faint decreases being even suggested, Figure 5), but

dx.doi.org/10.1021/pr500907d | J. Proteome Res. 2014, 13, 6033−6045

showed increases in the PUFA resonance (particularly in the case of DOX). The absence of neutral lipids increase, usually taken as an apoptosis sign and previously observed in DOX-treated melanoma (with 5 nM DOX),[27] leukemia (with 0.69 μM DOX)[24]), or breast and colon carcinomas cells (with 10 μM DOX),[26] suggests that no significant apoptosis is taking place in OS cells exposed to DOX or MTX in the conditions of this study. However, the increase in PUFA environments proportion (for both DOX and, to a lesser extent, MTX) and the knowledge that both drugs are known to ultimately induce apoptosis[7,8] indicates that apoptosis may be at earlier stages at the time of sampling (contrary to cDDP-treated cells).

Regarding phospholipid-related compounds, the changes in choline metabolites previously reported for cDDP have been confirmed with data reprocessing, but a relevant decrease in PE was newly observed. cDDP is believed to induce membrane breakdown in MG-63 cells, which leads to large and mild increases in GPC and Cho, respectively. Cho levels are possibly also affected by an involvement in enhanced phospholipid biosynthesis through PC formation or PTC-cycle regulation.[19] The GPC peak correlated positively with the PUFA resonance, through STOCSY (data not shown), which suggests a close metabolic link to phosphatidylcholine (PTC) hydrolysis, which possibly releases PUFAs into the cytosol and thus contributes to the NMR spectrum. It is important to note that STOCSY correlations between different compounds may either reflect metabolic links or be simply casual, ultimate confirmation of metabolic relationships requiring additional demonstration, for example, through specific pathway analysis. Regarding the elevated PC levels compared to controls (Figure S4), we propose that they are kept high through the activation of PE to PC conversion in order to sustain PTC synthesis, probably as an attempt to compensate for the concomitant membrane breakdown. The relatively elevated PC levels, except for 48 h, seem specific of cDDP action since relatively large PC decreases are observed for both DOX (Table 1, Figure S2) and MTX (Table 2, Figure S3), with no enhanced use of PE being noted (PE even shows a small increasing tendency, Table 1). For DOX, the variations in choline compounds differ from the reported information on other DOX-treated cells,[23,25,27] once more highlighting the dependence of drug effects on cell type. The lower PC levels were accompanied by large GPC and Cho increases, which reflect extensive membrane breakdown through phospholipases action. Lowered PC levels are usually associated with reduced PTC biosynthesis, accompanying cell growth arrest, and apoptosis[46] but may also arise from enhanced PC catabolism to Cho (probably more active than in cDDP, given the much larger Cho increase in DOX). Low PC levels have also been proposed to evidence inhibition of *de novo* biosynthesis of cytosolic lipids,[47] an effect possibly responsible for the lack of lipids increase in the DOX-treated cells. Furthermore, STOCSY analysis identified strong positive correlations between both GPC and Cho and the PUFA resonance (results not shown, $r > 0.7$), which again establishes a possible relationship between membrane degradation and an increased polyunsaturation degree in NMR-visible lipids. Since no concomitant increase in lipids occurs, this suggests that the proportion of cytosolic PUFA lipids is increasing, while keeping total lipids amount unchanged, through a mechanism that remains unclear at this stage. The above changes translate into clear decreases in the PC/GPC and PC/Cho ratios (Figure 5), the former having been related to cell growth arrest prior to apoptosis.[48] The distinctly different signature observed for MTX comprises a more marked decrease in PC than for DOX, reflecting a further decrease in PTC synthesis, and no meaningful changes in GPC or Cho (no significant membrane breakdown) in accordance with reports on MTX-treated breast cancer cells[25] and imatinib-treated leukemia cells.[49] These changes originate steadier decreases for PC/GCP and PC/Cho (Figure 5b), which establish a clear signature for MTX reflecting lower PTC synthesis (as for DOX) without concomitant membrane degradation (contrary to DOX).

Amino Acids

The previously reported large impact of cDDP on the amino acid metabolism of MG-63 cells[19] was presently confirmed, with much lower effects observed for DOX- and MTX-treated cells. For cDDP, the residually lower Tau levels (and the absence of measurable GSH changes) suggested a low level of oxidative stress (similarly to cDDP-treated lung cancer cells[14]), which probably justifies the efficiently leveled GSH contents. Since Glu and Gly are GSH precursors, through the γ-glutamyl cycle,[50] the concomitant decreases in both amino acids could also indicate some degree of activation of antioxidant protection mechanisms often associated with cell cycle arrest and apoptosis.[26,27,43,48,51] However, together with Ala decrease (also observed here, for cDDP), Gln/Glu reduction may also be indicative of enhanced tricarboxylic (TCA) cycle and oxidative phosphorylation activities in order to produce more ATP to sustain apoptosis.[27] In the OS cell line currently tested, this was not corroborated by variations in lactate or TCA cycle intermediates as seen in other studies,[48,49] but the decrease in Gly, Leu, Lys, Phe, Pro, and Tyr may arise from their enhanced catabolism through an activated TCA cycle, while acetate(s) may indicate a higher mithochondrial lipids β-oxidation activity. Finally, Val and Ile, not previously evaluated in cDDP-treated MG-63 cells, evolve against the general trend of amino acids decrease. STOCSY analysis (data not shown, $r > 0.7$) revealed positive correlations of these branched chain amino acids with a typical lipidic profile, possibly due to their catabolism crossing with the biosynthesis of branched chain fatty acids.

In DOX-treated cells, no relevant amino acid indicators of oxidative stress (decreases in Gln/Glu or Tau) were noted, although DOX induced a relevant decrease in GSH, which will be discussed in more detail. The absence of general amino acids depletion (with even a positive variation noted for Tyr) suggests no TCA cycle activation, although some kind of bioenergetic disturbance is noted through the increase in creatine, also reported to change in MG-63 spheroids exposed to radiation.[43] On the other hand, in MTX-treated cells, Tau and Glu are clearly decreased, which thus suggests oxidative stress enhancement accompanied by a small decreasing tendency in GSH. Furthermore, the noted increase in Gly, Tyr, and Phe (in contrast to cDDP) may stem from their underuse as anaplerotic agents to the TCA cycle and possibly indicate a slowing down of the energy metabolism, which is in agreement with the observed creatine depletion (opposite to DOX-treated cells).

Nucleotides and Other Compounds

The nucleotide base signatures are quite distinct between the three drugs presently tested, showing increases in UXP and UDP-GlcNAc species for cDDP and DOX and a marked Ado/Ino decrease apparently specific of cDDP-treated cells. The common increases may relate to the fact that both drugs exert their activity through their interaction with DNA and subsequent DNA conformational changes, but the different overall nucleotide profiles may relate to the different specific mechanisms involved. For MTX, the general absence of relevant

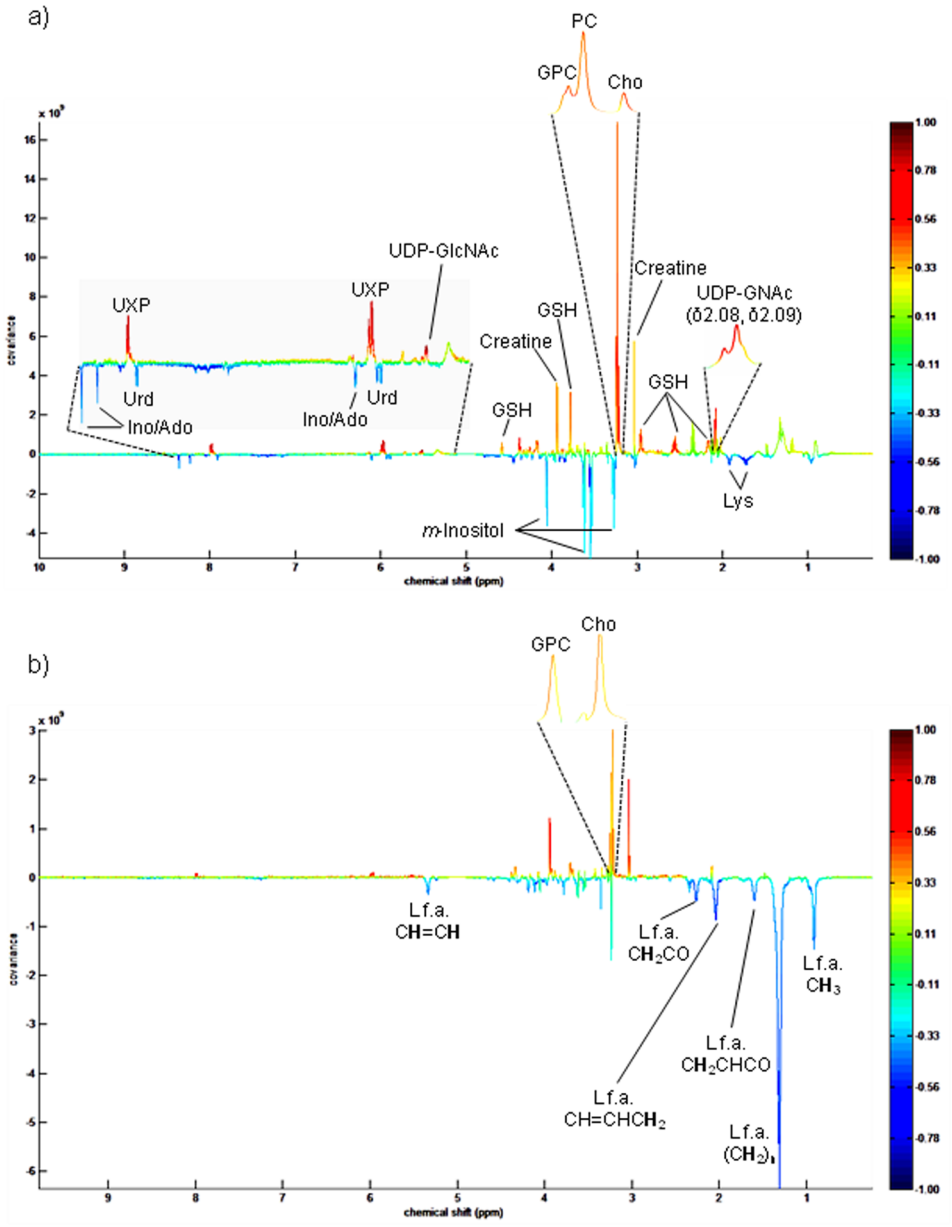

Figure 6. STOCSY results obtained for the UDP-GlcNAc resonance at δ 5.52 obtained for (a) cDDP-treated cells and in (b) DOX-treated cells.

changes (including for uridine, despite the apparent increase at 48 h) or decreasing tendencies (for Ado/Ino and UXP) are consistent with MTX being known to hamper *de novo* purine synthesis, probably keeping nucleotide levels low or unchanged, including those of pyrimidine bases (such as uridine and UXP). Specifically regarding UDP-GlcNAc, a donor in the glycosylation processes of post-translational proteins,[16,52] its increase was newly noted in this work in cDDP- and DOX-treated OS cells (remaining unchanged for MTX). This compound was previously seen to increase, along with UDP-GalNAc, in cDDP-treated brain tumor cells[16] and lung cancer cells[14] and was, in such studies, correlated to mobile lipids in association with apoptotic cell death. However, STOCSY analysis of our data (Figure 6a) revealed no correlation to lipid resonances in cDDP-treated OS cells and showed positive correlations with GPC, Cho and PC (membrane degradation metabolism), creatine, and GSH (antioxidative mechanism), with negative correlations seen with Lys, uridine, and Ado/Ino (the latter proposed to vary in relation to cDDP-induced DNA damage). In DOX-treated cells (Figure 6b), UDP-GlcNAc (much increased relatively to cDDP-treated cells) again correlated positively with the main membrane degradation products (GPC and Cho) and creatine but, notably, not to GSH, which thus suggests that in DOX-treated cells, the main metabolic origin of UDP-GlcNAc may not relate to antioxidative mechanisms as in cDDP. In addition, for DOX, UDP-GlcNAc actually correlated negatively with lipids, in agreement with the slight decreases seen for CH_3 and $(CH_2)_n$ resonances (Figure 5), which thus again contradicts a direct relationship with neutral lipids increase. Overall, the above observations suggest a general connection of UDP-GlcNAc with the active and preferential pathways of membrane degradation and energy metabolism (through creatine), while in cDDP, an additional link to cellular oxidative state and DNA degradation seems to exist.

Finally, some considerations are due on the marked *m*- and *s*-inositols decreases (*m*-inositol to a greater extent) seen for both

dx.doi.org/10.1021/pr500907d | J. Proteome Res. 2014, 13, 6033−6045

cDDP and DOX-treated cells, while no changes in these compounds were noted for MTX-treated cells. Depletion in *m*-inositol has been previously detected in several studies,[27,46,53] and such variation was assigned to several possible causes: disturbance in its osmolytic function through drug-induced partial inhibition of the Na^+/*m*-inositol cotransporter (SMIT);[46] diminished inhibition of the mitogen-activated protein kinase (MAPK) signal transduction pathway, thus leading to stimulation of cells into apoptosis;[46] effect on the biosynthesis and turnover of some phospholipids;[54] or activation of cell detoxification processes. To clarify the role of inositols in treated MG-63 cells (particularly upon cDDP and DOX treatments), STOCSY analysis of the inositol resonances (not shown) revealed that, in cDDP-treated cells, *m*-inositol decreases concomitantly with Tau, Glu/Gln, and creatine (besides *s*-inositol), whereas in DOX-treated cells, *m*-inositol decreases together with Glu/Gln and GSH (and *s*-inositol). These observations identified the marked inositol decreases as preferentially related with an ongoing antioxidative mechanism, although the corresponding metabolite signatures seem distinct.: (1) For cDDP, it is apparent that Tau, Glu/Gln, inositols, and possibly creatine help to regulate GSH levels efficiently (since such levels are unchanged upon drug treatment), and (2) for DOX, Glu/Gln and inositols alone seem to be insufficient to avoid a concomitant GSH use in the cellular response to oxidative stress (negative variation, Table 1). For MTX, the inositols resonances, although unchanged upon drug treatment, were found to also correlate weakly to Glu/Gln, GSH, and possibly creatine, which thus confirms the proposed link to an antioxidative response.

CONCLUSIONS

The effects of DOX, MTX, and cDDP on the metabolome of human OS MG-63 cells (at their IC_{50} concentration levels) were shown to be significantly distinct and provided valuable insight into the metabolic cellular responses to each of these anticancer drugs. While, cDDP-treated cells were characterized by membrane degradation and increase in neutral lipids, probably through *de novo* biosynthesis, DOX was found to induce more enhanced membrane degradation, accompanied by decreased PTC synthesis and apparent inhibition of *de novo* lipid synthesis. MTX treatment, in turn, evidenced no membrane degradation, while a marked decrease in PTC synthesis and possible inhibition of *de novo* lipid synthesis was observed. Therefore, assuming lipid changes as possible apoptosis markers, cDDP-treated cells may be undergoing apoptosis as apposed to DOX and MTX, which may, at their IC_{50} values, lead only to the earlier stages of cell arrest and apoptosis. Furthermore, apparent changes in the TCA cycle activity, oxidative stress, and nucleotide metabolism were noted. In particular, different degrees of cell response to oxidative stress were proposed, with apparent antioxidative metabolite signatures having been identified as comprising Tau, Glu/Gln *m*- and *s*-inositols, GSH, and possibly creatine as the main metabolite players. Furthermore, for cDDP and DOX, a specific connection was found between UDP-GlcNAc and the active pathways of membrane degradation and energy metabolism (through creatine), with an additional link to oxidative state (GSH) and DNA degradation (Ado/Ino and uridine) seen for cDDP, which is in accordance with the recognized mechanism of action of this compound.

These results illustrate the extent of detailed information obtainable through NMR metabolomics, identifying metabolic nuances in the response of MG-63 cells to different anticancer drugs, often used together in the clinic. Studying their specific metabolic impact is the first step toward the understanding (at the molecular level) of their synergetic effects, which is determinant in defining new clinical biomarkers of drug efficacy and treatment monitoring.

ASSOCIATED CONTENT

Supporting Information

Average 700 MHz ^{1}H HRMAS spectra of MG-63 cells at 48 h and corresponding multivariate analysis results; time course plots of peak areas as a function of time for the assays performed with DOX, MTX, and cDDP; and Monte Carlo Cross-Validation (MCCV) results of PLS-DA models obtained for to the assays with DOX, MTX, and cDDP. This material is available free of charge via the Internet at http://pubs.acs.org.

AUTHOR INFORMATION

Corresponding Author

*E-mail: agil@ua.pt. Phone: +351 234 370707. Fax: +351 234 370084.

Notes

The authors declare no competing financial interest.

ACKNOWLEDGMENTS

The authors acknowledge funding from the European Regional Development Fund-FEDER through the Competitive Factors Thematic Operational Programme-COMPETE and the Foundation for Science and Technology-FCT, Portugal (CICECO-FCOMP-01-0124-FEDER-037271, PEst-OE/QUI/UI0070/2014, PEst-C/CTM/LA0011/2013, PTDC/SAL-BEB-66896/2006, and SFRH/BD/63916/2009). The Portuguese National NMR Network (RNRMN), supported with FCT funds, is acknowledged (particularly for access to 800 MHz NMR equipment). The authors thank M. Spraul, Bruker BioSpin, Germany, for access to software and spectral databases, and the Associate Laboratory IBMC-INEB for kindly providing the MG-63 cell line.

REFERENCES

(1) Cuperlovic-Culf, M.; Barnett, D. A.; Culf, A. S.; Chute, I. Cell Culture Metabolomics: Applications and Future Directions. *Drug Discovery Today* **2010**, *15*, 610−621.

(2) D'Alessandro, A.; Zolla, L. Proteomics and Metabolomics in Cancer Drug Development. *Expert Rev. Proteomics* **2013**, *10*, 473−488.

(3) Chiaradonna, F.; Moresco, R. M.; Airoldi, C.; Gaglio, D.; Palorini, R.; Nicotra, F.; Messa, C.; Alberghina, L. From Cancer Metabolism to New Biomarkers and Drug Targets. *Biotechnol. Adv.* **2012**, *30*, 30−51.

(4) Ta, H. T.; Dass, C. R.; Choong, P. F. M.; Dunstan, D. E. Osteosarcoma Treatment: State of the Art. *Cancer Metastasis Rev.* **2009**, *28*, 247−263.

(5) Luetke, A.; Meyers, P. A.; Lewis, I.; Juergens, H. Osteosarcoma Treatment—Where Do We Stand? A Sate of the Art Review. *Cancer Treat. Rev.* **2014**, *40*, 523−532.

(6) Longhi, A.; Errani, C.; Paolis, M. D.; Mercuri, M.; Bacci, G. Primary Bone Osteosarcoma in the Pediatric Age: State of the Art. *Cancer Treat. Rev.* **2006**, *32*, 423−436.

(7) Minotti, G.; Menna, P.; Salvatorelli, E.; Cairo, G.; Gianni, L. Anthracyclines: Molecular Advances and Pharmacologic Developments in Antitumor Activity and Cardiotoxicity. *Pharmacol. Rev.* **2004**, *56*, 185−229.

(8) Schmiegelow, K. Advances in Individual Prediction of Methotrexate Toxicity: A Review. *Br. J. Haematol.* **2009**, *146*, 489−503.

(9) Wang, D.; Lippard, S. J. Cellular Processing of Platinum Anticancer Drugs. *Nat. Rev. Drug Discovery* **2005**, *4*, 307−320.

(10) Kelland, L. The Resurgence of Platinum-Based Cancer Chemotherapy. *Nat. Rev. Cancer* **2007**, *7*, 573−584.
(11) Tsang, R. Y.; Al-Fayed, T.; Au, H. J. Cisplatin Overdose: Toxicities and Management. *Drug Saf.* **2009**, *32*, 1109−1022.
(12) Ahmad, S. Platinum-DNA Interactions and Subsequent Cellular Processes Controlling Sensitivity to Anticancer Platinum Complexes. *Chem. Biodiversity* **2010**, *7*, 543−566.
(13) Huang, Z.; Tong, Y.; Wang, J.; Huang, Y. NMR Studies of the Relationship Between the Changes of the Membrane Lipids and the Cisplatin-Resistance of A549/DDP Cells. *Cancer Cell Int.* **2003**, *3*, 5.
(14) Duarte, I. F.; Ladeirinha, A. F.; Lamego, I.; Gil, A. M.; Carvalho, L.; Carreira, I. M.; Melo, J. B. Potential Markers of Cisplatin Treatment Response Unveiled by NMR Metabolomics of Human Lung Cells. *Mol. Pharmaceutics* **2013**, *10*, 4242−4251.
(15) Lindskog, M.; Spenger, C.; Jarvet, J.; Graslund, A.; Kogner, P. Predicting Resistance or Response to Chemotherapy by Proton Magnetic Resonance Spectroscopy in Neuroblastoma. *J. Nat. Cancer Inst.* **2004**, *96*, 1457−1466.
(16) Pan, X.; Wilson, M.; Mirbahai, L.; McConville, C.; Arvanitis, T. N.; Griffin, J. L.; Kauppinen, R. A.; Peet, A. C. In Vitro Metabonomic Study Detects Increases in UDP-GlcNAc and UDP-GalNAc as Early Phase Markers of Cisplatin Treatment Response in Brain Tumor Cells. *J. Proteome Res.* **2011**, *10*, 3493−3500.
(17) Pan, X.; Wilson, M.; McConville, C.; Arvanitis, T. N.; Griffin, J. L.; Kauppinen, R. A.; Peet, A. C. Increased Unsaturation of Lipids in Cytoplasmic Lipid Droplets in DAOY Cancer Cells in Response to Cisplatin Treatment. *Metabolomics* **2013**, *9*, 722−729.
(18) Liu, S.; Wang, W.; Zhou, X.; Gu, R.; Ding, Z. Dose Responsive Effects of Cisplatin in L02 Cells Using NMR-Based Metabolomics. *Environ. Toxicol. Pharmacol.* **2014**, *37*, 150−157.
(19) Duarte, I. F.; Lamego, I.; Marques, J.; Marques, M. P.; Blaise, B. J.; Gil, A. M. Nuclear Magnetic Resonance (NMR) Study of the Effect of Cisplatin on the Metabolic Profile of MG-63 Osteosarcoma Cells. *J. Proteome Res.* **2010**, *9*, 5877−5886.
(20) Moyec, L. L.; Tatoud, R.; Degeorges, A.; Calabresse, C.; Bauza, G.; Eugene, M.; Calvo, F. Proton Nuclear Magnetic Resonance Spectroscopy Reveals Cellular Lipids Involved in Resistance to Adriamycin and Taxol by the K562 Leukemia Cell Line. *Cancer Res.* **1996**, *56*, 3461−3467.
(21) Blankenberg, F. G.; Katsikis, P. D.; Storrs, R. W.; Beaulieu, C.; Spielman, D.; Chen, J. Y.; Naumovski, L.; Tait, J. F. Quantitative Analysis of Apoptotic Cell Death Using Proton Nuclear Magnetic Resonance Spectroscopy. *Blood* **1997**, *89*, 3778−3786.
(22) Ronen, S. M.; DiStefano, F.; McCoy, C. L.; Robertson, D.; Smith, T. A. D.; Al-Saffar, N. M.; Titley, J.; Cunningham, D. C.; Griffiths, J. R.; Leach, M. O.; Clarke, P. A. Magnetic Resonance Detects Metabolic Changes Associated with Chemotherapy-Induced Apoptosis. *Br. J. Cancer* **1999**, *80*, 1035−1041.
(23) Le Moyec, L.; Legrand, O.; Larue, V.; Kawakami, M.; Marie, J. P.; Calvo, F.; Hantz, E.; Taillandier, E. Magnetic Resonance Spectroscopy of Cellular Lipid Extracts from Sensitive, Resistant, and Reverting K562 Cells and Flow Cytometry for Investigating the P-Glycoprotein Function in Resistance Reversion. *NMR Biomed.* **2000**, *13*, 92−101.
(24) Rainaldi, G.; Romano, R.; Indovina, P.; Ferrante, A.; Motta, A.; Indovina, P. L.; Santini, M. T. Metabolomics Using 1H-NMR of Apoptosis and Necrosis in HL60 Leukemia Cells: Differences Between the Two Types of Cell Death and Independence from the Stimulus of Apoptosis Used. *Radiat. Res.* **2008**, *169*, 170−180.
(25) Sterin, M.; Cohen, J. S.; Mardor, Y.; Berman, E.; Ringel, I. Levels of Phospholipid Metabolites in Breast Cancer Cells Treated with Antimitotic Drugs: A ^{31}P-Magnetic Resonance Spectroscopy Study. *Cancer Res.* **2001**, *61*, 7536−7543.
(26) Santini, M. T.; Romano, R.; Rainaldi, G.; Filippini, P.; Bravo, E.; Porcu, L.; Motta, A.; Calcabrini, A.; Meschini, S.; Indovina, P. L.; Arancia, G. The Relationship Between ^{1}H-NMR Mobile Lipid Intensity and Cholesterol in Two Human Tumor Multidrug Resistant Cell Lines (MCF-7 and LoVo). *Biochim. Biophys. Acta* **2001**, *1531*, 111−131.
(27) Triba, M. N.; Starzec, A.; Bouchemal, N.; Guenin, E.; Perret, G. Y.; Le Moyec, L. Metabolomic Profiling with NMR Discriminates Between Biphosphonate and Doxorubicin Effects on B16 Melanoma Cells. *NMR Biomed.* **2010**, *23*, 1009−1016.
(28) Miura, D.; Fujimura, Y.; Tachibana, H.; Wariishi, H. Highly Sensitive Matrix-Assisted Laser Desorption Ionization-Mass Spectrometry for High-Throughput Metabolic Profiling. *Anal. Chem.* **2010**, *82*, 498−504.
(29) Myint, K. T.; Uehara, T.; Aoshima, K.; Oda, Y. Polar Anionic Metabolome Analysis by Nano-LC/MS with a Metal Chelating Agent. *Anal. Chem.* **2009**, *81*, 7766−7772.
(30) Uehara, T.; Yokoi, A.; Aoshima, K.; Tanaka, S.; Kadowaki, T.; Tanaka, M.; Oda, Y. Quantitative Phosphorous Metabolomics Using Nanoflow Liquid Chromatography−Tandem Mass Spectrometry and Culture-Derived Comprehensive Global Internal Standards. *Anal. Chem.* **2009**, *81*, 3836−3842.
(31) Dieterle, F.; Ross, A.; Schlotterbeck, G.; Senn, H. Probabilistic Quotient Normalization as Robust Method To Account for Dilution of Complex Biological Mixtures. Application in ^{1}H NMR Metabonomics. *Anal. Chem.* **2006**, *78*, 4281−4290.
(32) Berridge, M. V.; Tan, A. S. Characterization of the Cellular Reduction of 3-(4,5-Dimethylthiazol-2-yl)-2,5-diphenyltetrazolium Bromide (MTT): Subcellular Localization, Substrate Dependence, and Involvement of Mitochondial Electron Transport in MTT Reduction. *Arch. Biochem. Biophys.* **1993**, *303*, 474−482.
(33) Mosmann, T. Rapid Colorimetric Assay for Cellular Growth and Survival: Application to Proliferation and Cytotoxicity Assays. *J. Immunol. Methods* **1983**, *65*, 55−63.
(34) Wishart, D. S.; Jewison, T.; Guo, A. C.; Wilson, M.; Knox, C.; Liu, Y.; Djoumbou, Y.; Mandal, R.; Aziat, F.; Dong, E.; Douatra, S.; Sinelnikov, I.; Arndt, D.; Xia, J.; Liu, P.; Yallou, F.; Bjorndahl, T.; Perez-Pineiro, R.; Eisner, R.; Allen, F.; Neveu, V.; Greiner, R.; Scalbert, A. HMDB 3.0—The Human Metabolome Database in 2013. *Nucleic Acids Res.* **2013**, *41*, D801−807.
(35) Cloarec, O.; Dumas, M. E.; Craig, A.; Barton, R. H.; Trygg, J.; Hudson, J.; Blancher, C.; Gauguier, D.; Lindon, J. C.; Holmes, E.; Nicholson, J. Statistical Total Correlation Spectroscopy: An Exploratory Approach for Latent Biomarker Identification from Metabolomic H-1 NMR Data Sets. *Anal. Chem.* **2005**, *77*, 1282−1289.
(36) Veselkov, K. A.; Lindon, J. C.; Ebbels, T. M. D.; Crockford, D.; Volynkin, V. V.; Holmes, E.; Davies, D. B.; Nicholson, J. K. Recursive Segment-Wise Peak Alignment of Biological H-1 NMR Spectra for Improved Metabolic Biomarker Recovery. *Anal. Chem.* **2009**, *81*, 56−66.
(37) Berben, L.; Sereika, S. M.; Engberg, S. Effect Size Estimation: Methods and Examples. *Int. J. Nurs. Stud.* **2012**, *49*, 1039−1047.
(38) Hakumäki, J. M.; Kauppinen, R. A. ^{1}H NMR Visible Lipids in the Life and Death of Cells. *Trends Biochem. Sci.* **2000**, *25*, 357−362.
(39) Delikatny, E. J.; Chawla, S.; Leung, D.-J.; Poptani, H. MR-Visible Lipids and the Tumor Microenvironment. *NMR Biomed.* **2011**, *24*, 592−611.
(40) Mannechez, A.; Reungpatthanaphong, P.; de Certaines, J. D.; Leray, G.; Le Moyec, L. Proton NMR Visible Mobile Signals in Sensitive and Multidrug-Resistant K562 Cells Are Modulated by Lipid Rafts. *Cancer Cell Int.* **2005**, *5*, 2.
(41) Boren, J.; Brindle, K. M. Apoptosis-Induced Mitochondrial Dysfunction Causes Cytoplasmic Lipid Droplet Formation. *Cell Death Differ.* **2012**, *19*, 1561−1570.
(42) Milkevitch, M.; Shim, H.; Pilatus, U.; Pickup, S.; Wehrle, J. P.; Samid, D.; Poptani, H.; Glickson, J. D.; Delikatny, E. J. Increases in NMR-Visible Lipid and Glycerophosphocholine During Phenylbutyrate-Induced Apoptosis in Human Prostate Cancer Cells. *Biochim. Biophys. Acta* **2005**, *1734*, 1−12.
(43) Santini, M. T.; Romano, R.; Rainaldi, G.; Ferrante, A.; Motta, A.; Indovina, P. L. Increases in ^{1}H-NMR Mobile Lipids Are Not Always Associated with Overt Apoptosis: Evidence from MG-63 Human Osteosarcoma Three-Dimensional Spheroids Exposed to a Low Dose (2 Gy) of Ionizing Radiation. *Radiat. Res.* **2006**, *165*, 131−141.
(44) Mirbahai, L.; Wilson, M.; Shaw, C. S.; McConville, C.; Malcomson, R. D. G.; Kauppinen, R. A.; Peet, A. C. Lipid Biomarkers

of Glioma Cell Growth Arrest and Cell Death Detected by ^{1}H Magic Angle Spinning MRS. *NMR Biomed.* **2012**, *25*, 1253−1262.
(45) Zietkowski, D.; Payne, G. S.; Nagy, E.; Mobberley, M. A.; Ryder, T. A.; De Souza, N. M. Comparison of NMR Lipid Profiles in Mitotic Arrest and Apoptosis as Indicators of Paclitaxel Resistance in Cervical Cell Lines. *Magn. Reson. Med.* **2012**, *68*, 369−377.
(46) Knijn, A.; Brisdelli, F.; Ferretti, A.; Iorio, E.; Marcheggiani, D.; Bozzi, A. Metabolic Alterations in K562 Cells Exposed to Taxol and Tyrphostin AG957: ^{1}H NMR and Biochemical Studies. *Cell Biol. Int.* **2005**, *29*, 890−897.
(47) Ross, J.; Najjar, A. M.; Sankaranarayanapillai, M.; Tong, W. P.; Kaluarachchi, K.; Ronen, S. M. Fatty Acid Synthase Inhibition Results in a Magnetic Resonance-Detectable Drop in Phosphocholine. *Mol. Cancer. Ther.* **2008**, *7*, 2556−2565.
(48) Mirbahai, L.; Wilson, M.; Shaw, C. S.; McConville, C.; Malcomson, R. D.; Griffin, J. L.; Kauppinen, R. A.; Peet, A. C. ^{1}H Magnetic Resonance Spectroscopy Metabolites as Biomarkers for Cell Cycle Arrest and Cell Death in Rat Glioma Cells. *Int. J. Biochem. Cell Biol.* **2011**, *43*, 990−1001.
(49) Klawitter, J.; Anderson, N.; Klawitter, J.; Christians, U.; Leibfritz, D.; Eckhardt, S. G.; Serkova, N. J. Time-Dependent Effects of Imatinib in Human Leukaemia Cells: A Kinetic NMR-Profiling Study. *Br. J. Cancer* **2009**, *100*, 923−931.
(50) Macnicol, P. K. Homoglutathione and Glutathione Synthetases of Legume Seedlings: Partial Purification and Substrate Specificity. *Plant Sci.* **1987**, *53*, 229−235.
(51) García-Álvarez, I.; Fernández-Mayoralas, A.; Garrido, L. Effect of Drugs in Cells and Tissues by NMR Spectroscopy. *Curr. Top. Med. Chem.* **2011**, *11*, 27−42.
(52) Grande, S.; Palma, A.; Luciani, A. M.; Rosi, A.; Guidoni, L.; Viti, V. Glycosidic Intermediates Identified in H-1 MR Spectra of Intact Tumour Cells May Contribute to the Clarification of Aspects of Glycosylation Pathways. *NMR Biomed.* **2011**, *24*, 68−79.
(53) Griffin, J. L.; Pole, J. C. M.; Nicholson, J. K.; Carmichael, P. L. Cellular Environment of Metabolites and a Metabonomic Study of Tamoxifen in Endometrial Cells Using Gradient High Resolution Magic Angle Spinning ^{1}H NMR Spectroscopy. *Biochim. Biophys. Acta* **2003**, *1619*, 151−158.
(54) Ferretti, A.; D'Ascenzo, S.; Knijn, A.; Iorio, E.; Dolo, V.; Pavan, A.; Podo, F. Detection of Polyol Accumulation in a New Ovarian Carcinoma Cell Line, CABA I: A ^{1}H NMR study. *Br. J. Cancer* **2002**, *86*, 1180−1187.